Precision determination of the fine-structure interval in the ground state of positronium. III*

E. R. Carlson,† V. W. Hughes, and I. Lindgren‡
Gibbs Laboratory, Physics Department, Yale University, New Haven, Connecticut 06520
(Received 13 January 1976)

With an improved microwave magnetic resonance apparatus the Zeeman transition in orthopositronium has been remeasured and hence the ground-state fine-structure interval $\Delta\nu$ in positronium has been determined with higher precision: $\Delta\nu = 203.384 \pm 0.004$ GHz (20 ppm). The measurements were made in N_2 gas and gave the value $(1/\Delta\nu)\partial(\Delta\nu)/\partial D = (-5.7 \pm 1.4) \times 10^{-5}$ atm^{-1} at 23°C for the coefficient of the fine-structure density shift. Relativistic binding corrections to the positronium Zeeman transition were taken into account.

I. INTRODUCTION

Positronium (e^+e^-) has long been recognized as an ideal atomic system for testing quantum electrodynamics (QED),[1,2,3,4] and in particular the Bethe-Salpeter equation for the bound-state lepton-antilepton system.

The ground state of positronium is split into two fine structure levels designated $^3S_1$ (orthopositronium) and $^1S_0$ (parapositronium). The same basic method has been used thus far in all precision measurements of the fine structure interval $\Delta\nu$. Positronium in the ground state is formed by stopping positrons from a radioactive source in a high-purity gas. Zeeman transitions are induced between the $M = \pm 1$ and $M = 0$ magnetic substates of orthopositronium, and are observed through the change in the annihilation radiation. The resonance line is obtained by varying the magnetic field with fixed microwave frequency. As yet no study has been made of the direct $\Delta\nu$ transition, principally because of the technical difficulties associated with the required high microwave power and high-frequency system at the $\Delta\nu$ frequency of 203 GHz; furthermore, there is no fundamental disadvantage to determining $\Delta\nu$ from the Zeeman transition, because the ratio of the natural radiative width to the transition frequency is the same for the Zeeman transition and the direct $\Delta\nu$ transition.

This paper, designated paper III, reports on the third in a series of precision measurements of $\Delta\nu$ done first at Columbia and then at Yale. The results of Hughes, Marder, and Wu,[5] who measured $\Delta\nu$ to a precision of 200 ppm were presented in paper I. Significant improvements in experimental technique by Theriot, Beers, Hughes, and Ziock,[6] which permitted them to achieve a 60 ppm precision in $\Delta\nu$, were described in paper II. In the present experiment, design improvements allow a precision of 20 ppm in $\Delta\nu$ to be obtained. A new, larger magnet is used, which produces a more homogeneous magnetic field and also allows positronium to be observed over a larger volume, thus increasing the signal counting rate. Another increase in the counting rate is accomplished by using four coincidence detectors. Nitrogen is used as the stopping gas because it supports larger microwave fields than argon, which was used for paper II, and thus allows the production of adequate signals at lower gas pressure. Brief reports of this research have been published.[7,8] A subsequent measurement[9,10] of $\Delta\nu$ with a precision of 6 ppm is the subject of the following paper IV. Comparison of our results with other measurements of $\Delta\nu$ is given in paper IV.

In the present paper III, Sec. II gives current material on the theory of the experiment to supplement that of paper II, Sec. III describes the new experimental apparatus, Sec. IV presents the data analysis, and Sec. V gives the results.

II. THEORY OF THE EXPERIMENT

The theory of the experiment was discussed rather completely in Paper II. Here we principally give current supplementary material and define quantities required for this Paper III and for Paper IV.

A. Energy eigenvalues

The theoretical expression for $\Delta\nu$ is[10,11,12,13,14]

$$\Delta\nu = \tfrac{1}{2}\alpha^2 c\mathcal{R}\left[\tfrac{7}{3} - (\alpha/\pi)\left(\tfrac{32}{9} + 2\ln 2\right) + \alpha^2 \ln\alpha^{-1}\right]$$
$$= 203.404\,117\,(86)\ \text{GHz}[0.42\ \text{ppm}],$$
$$\alpha^{-1} = 137.035\,987\,(29),\ [0.21\ \text{ppm}]^{15}, \qquad (1)$$
$$\mathcal{R} = 1.097\,373\,143\,(10) \times 10^5\ \text{cm}^{-1},\ [0.010\ \text{ppm}]^{16},$$
$$c = 299\,792\,458\,(1.2)\ \text{m/sec},\ [0.004\ \text{ppm}]^{17}.$$

The indicated uncertainty in $\Delta\nu$ is due to the uncertainties in the values of the fundamental constants, and indeed principally in the value of α.

The Zeeman energy levels as a function of magnetic field[6] are shown in Fig. 1, in which M is the magnetic quantum number. The quantity which is directly measured in our experiment is the Zeeman transition frequency f_{01} between the $M=0$ and $M=\pm 1$ magnetic sublevels of orthopositronium:

$$f_{01} = (\tfrac{1}{2}\Delta\nu)[(1+x^2)^{1/2} - 1], \tag{2}$$

where $x = 2g'\mu_B H_0/h\Delta\nu$. The quantity g' is the gyromagnetic ratio of the electron bound in positronium[18,19,20] and is given by

$$g' = g_-(1 - \tfrac{5}{24}\alpha^2) = g_-(1 - 11.1\times 10^{-6}), \tag{3}$$

in which g_- is the g value of the free electron and the effect of binding is given by the α^2 term. The current theoretical value for g_- is[21,22]

$$\begin{aligned} g_- &= 2[1 + \alpha/2\pi - 0.328\,48(\alpha/\pi)^2 \\ &\quad + (1.195 \pm 0.026)(\alpha/\pi)^3] \\ &= 2[1.001\,159\,652\,5(5)], \end{aligned} \tag{4}$$

in which the value of α given above is used.

B. Annihilation

The current theoretical values for the annihilation rates of parapositronium[23] into 2γ rays, λ_p, and of orthopositronium[24] into 3γ rays, λ_0, are

$$\begin{aligned} \lambda_p &= \frac{\alpha^5 mc^2}{2\hbar}\left[1 - \frac{\alpha}{\pi}\left(5 - \frac{\pi^2}{4}\right)\right] \\ &= 0.798\times 10^{10}\ \text{sec}^{-1}, \end{aligned} \tag{5}$$

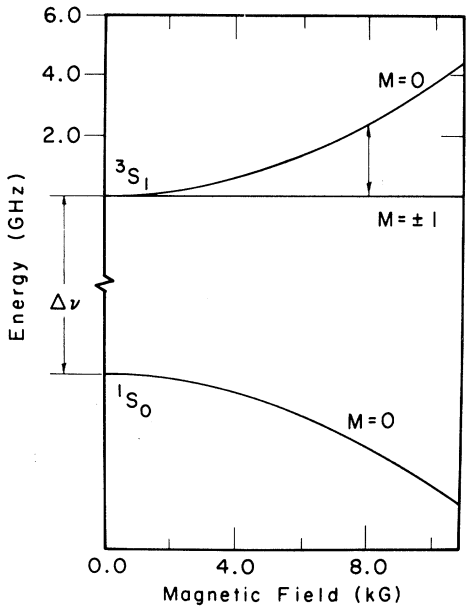

FIG. 1. Zeeman energy levels of positronium in its ground state.

$$\begin{aligned} \lambda_0 &= \frac{\alpha^6 mc^2}{\hbar}\left(\frac{2}{9\pi}\right)(\pi^2 - 9)\left(1 + \frac{\alpha}{\pi}(1.86 \pm 0.45)\right) \\ &= (0.724 \pm 0.001)\times 10^7\ \text{sec}^{-1}. \end{aligned} \tag{6}$$

In a magnetic field the annihilation rates of the magnetic substates (J,M) of orthopositronium become

$$\lambda_{1,1} = \lambda_{1,-1} = \lambda_0, \tag{7}$$

$$\lambda_{1,0} = \lambda_{10,3} + \lambda_{10,2}. \tag{8}$$

For x small, the three-photon annihilation rate of $(1,0)$ is

$$\lambda_{10,3} \simeq (1 - \tfrac{1}{4}x^2)\lambda_0, \tag{9}$$

and its two photon annihilation rate is

$$\lambda_{10,2} \simeq \tfrac{1}{4}x^2\lambda_p. \tag{10}$$

Hence the branching ratio of state $(1,0)$ for annihilation into 2γ and 3γ is

$$B_{1,0} = \lambda_{10,2}/\lambda_{10,3} \simeq \tfrac{1}{4}x^2\lambda_p/\lambda_0. \tag{11}$$

C. Theoretical line shape

The signal S measured in the experiment is proportional to the number of orthopositronium atoms which decay by two quantum annihilation due to the microwave field

$$S \propto (P_{1,0} + P_{-1,0} + P_{0,0} - \lambda_{10,2}/\lambda_{1,0}), \tag{12}$$

where $P_{M,0}$ is the probability of two-photon annihilation for an atom initially in the $(1,M)$ substate of orthopositronium, derived in paper II.

Under the conditions of small x and low microwave power, the line shape of Eq. (12) reduces to a power broadened Lorentzian in the magnetic field, H_0.

$$S \propto \frac{AH_1^2}{(H_0 - H_{0r})^2 + B^2}, \tag{13}$$

where the constants A and B have been defined in Paper II, H_1 is the magnitude of the microwave magnetic field, H_{0r} is value of the static magnetic field at resonance.

The approximate resonance line shape given by Eq. (13) is not entirely adequate to represent the experimental line to the desired accuracy of the measurement. Deviations of the approximate shape from the complete theory are small, however, so that Eq. (13) could be used for part of the data analysis, for which its simple form had computational advantages.

The effects of collision processes on the line shape have been treated by the methods of paper I and II. One important effect is line broadening from the increase in the effective annihilation rate of orthopositronium in nitrogen due to posi-

tron annihilation during collisions. For positronium in nitrogen the annihilation rate has been measured to be[25]

$$\lambda_0(N_2) = \lambda_0(1 + 0.029P)\,, \tag{14}$$

where P is the nitrogen pressure in atmospheres. A second important effect is the fine structure density shift which will be discussed in Sec. IV.

III. EXPERIMENTAL APPARATUS

The experimental apparatus (Fig. 2) was divided functionally into several systems: electromagnet, microwave cavity and generator, positron source, gas-handling system, and γ-ray detectors and electronics.

A. Magnetic field

The magnetic field H_0 was produced by an electromagnet[26] with tapered ring-shim pole pieces and a 10.6-cm air gap. The field was regulated by a nuclear magnetic resonance system[27] (Fig. 3). The transmitter was a frequency synthesizer with frequency stability better than 0.1 ppm over the time periods during which data were taken. With the magnet cooling water controlled to ±0.25°C and with much of the surface area of the yoke covered with thermal insulation, the stability of the magnetic field when controlled by this system was observed to be better than 0.5 ppm.

The NMR probe was a 6-mm-diam spherical glass sample holder potted in epoxy to provide a cylindrical shape on which an rf coil and a pair of sweep coils were wound. The linewidth of the mineral oil sample[28] was 25 mG at 7.8 kG, or about 3 ppm. By comparison in a high-resolution NMR spectrometer,[29] the NMR frequency of protons in the sample material was found to be 3.7-ppm smaller than the NMR frequency of protons in pure water at the same field, in agreement with the published values of -3.4 ± 0.5 ppm[30] and -3.7 ± 0.6 ppm.[31] A correction for bulk diamagnetism was not required because the sample holder was spherical.[32]

During data taking, the magnetic field was measured with an NMR probe located in one lid of the microwave cavity. The difference in the magnetic fields at the probe location and at the center of the cavity where positronium was observed was measured with two NMR systems. The field at the center was 4.6 ± 1.0-ppm lower than at the probe location. Thus the measured NMR frequency is 0.9-ppm higher than that of a pure water sample at the cavity center.

Measurements of the homogeneity of the magnetic field were made using two NMR systems, one with a fixed probe to regulate the field and the other with a probe mounted on a positioning device. The NMR sample for regulation was D_2O doped with $GdCl_3$, and the movable NMR sample was mineral oil; different nuclei were used to avoid interference. A magnetic field plot for a

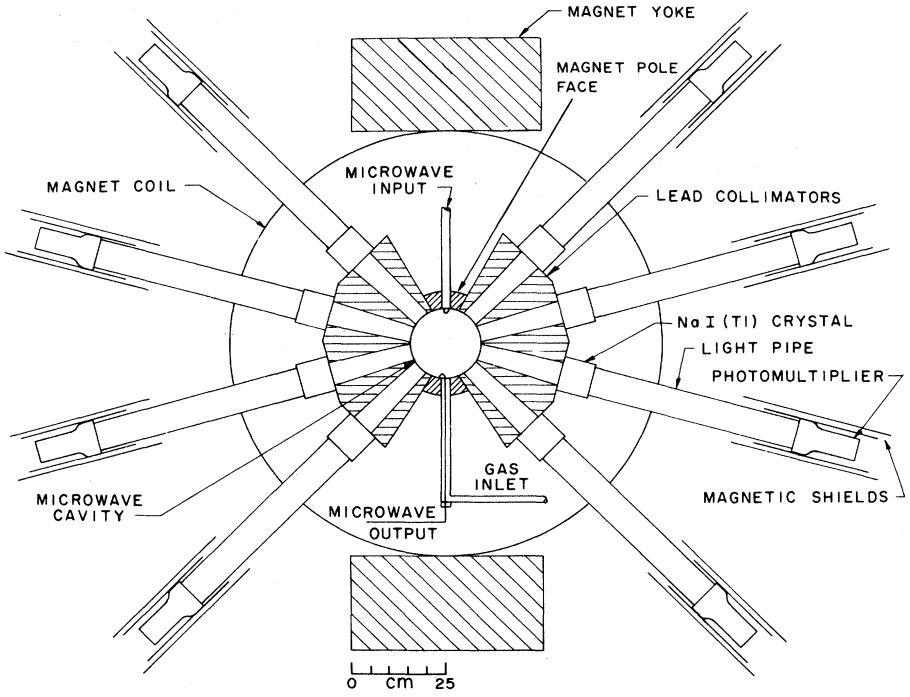

FIG. 2. Schematic diagram of the experimental apparatus.

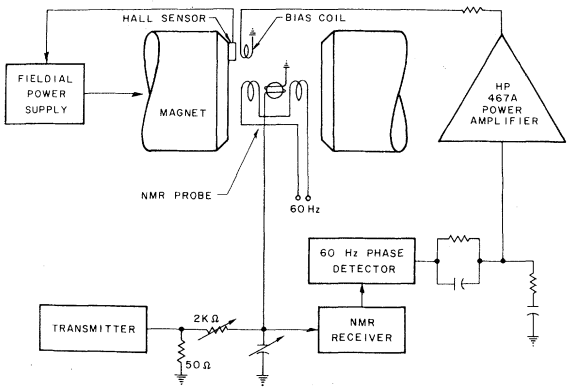

FIG. 3. Block diagram of the nuclear magnetic resonance circuit for magnetic field regulation.

central field of 7.80 kG is shown in Fig. 4. The total field variation over the region in which positronium annihilations were observed, which was a cylinder 2.5 cm in diam and 2.5-cm long at the center of the magnet, was 47 mG or 6 ppm. The plots taken before and after data-taking were the same to within ±1 mG.

B. Microwave system

A block diagram of the microwave system is shown in Fig. 5.

The frequency generation started with a frequency of about 29.0 MHz produced by a frequency synthesizer.[33] The crystal oscillator in the synthesizer was adjusted to within 1 part in 10^{10} of its nominal value of 1 MHz by comparison with the National Bureau of Standards time signals on WWVB. (This oscillator was used as the reference for all frequency measurements in the experiment.) The synthesizer output was multiplied to 2.32 GHz in two stages and then leveled with a PIN diode modulator. The leveled 2.32 GHz signal was amplified to 200–500 W by a klystron amplifier.[34] The synthesized frequency was adjusted to the resonant frequency of the cavity, which varied with gas pressure and cavity temperature. The microwave frequency was stable to 2 parts in 10^7 over the 6-h period of a pass through the resonance line.

The spectral purity of the microwave output was sufficiently good that only the passband of the i.f. filter in the spectrum analyzer used for the purity measurement was observed. The filter passband provided a worst case estimate of the spectral purity: 1-kHz wide (±0.25 ppm) at −3 dB, and 5-kHz wide (±1.25 ppm) at −38 dB.

The microwave cavity (Fig. 6) was fabricated from oxygen-free high-conductivity copper and was silver-plated. It was constructed in three pieces, a flanged body and two lids, and a seal was formed between the body and each lid with indium-silver metal O rings. The cavity interior was a right circular cylinder 15.73 cm in diam and 7.30-cm high. Much of the body wall between flanges was cut to a thickness of 0.25 cm to improve γ-ray transmission. The cavity was designed to operate over a pressure range of 10^{-6} Torr to 6 atm. A hole 1.08 cm in diam and 0.64-cm deep was bored in the center of the inside face of one lid to serve as a receptacle for the positron source holder. The hole acted as a waveguide beyond cutoff and protected the source from microwave heating. A 0.71-cm diam hole was bored along a diameter in each lid to permit insertion of an NMR probe so that the NMR sample was centered on the axis of the cavity. Cooling water with its temperature controlled to ±0.25°C was circulated through passages in the cavity.

Power was coupled into the cavity by a 20-cm length of 1.0-cm o.d. semirigid coaxial cable (UT-390) with a loop on one end. The necessary pressure seal was formed by swaging to the cable a 1.0-cm tube fitting, which had been bored out to permit the cable to pass through. Repeated fine adjustment of the coupling could be made by rotating the cable before final tightening of the fitting, and the voltage-standing wave ratio (VSWR) on the input line was less than 1.15.

Another coupling loop was mounted on the cavity opposite the input coupler to sample the fields in the cavity for the power leveling system described below. This loop was greatly undercoupled because very little power was needed to drive the leveling circuit.

The cavity was operated in the TM_{110} mode which produced a microwave magnetic field which was linearly polarized perpendicular to the static magnetic field, was independent of position along the z axis (the cavity cylinder axis), and was constant to within 6.5% over the 2.5-cm diam region in which positronium was observed. The resonant frequency of the cavity in the TM_{110} mode was 2.32 GHz. The cavity Q was determined by measuring the VSWR at the cavity input as a function of frequency,[35] and the value for the loaded Q was $Q_L = 13\,700 \pm 20\%$. From the measured input power to the cavity and the Q of the cavity, the amplitude H_1 of the microwave magnetic field at the center of the cavity can be computed as is done later for Table I.

The fields inside the cavity were sampled by the pickup loop which transmitted a small amount of power to a crystal detector. The output of the detector was compared with a reference voltage, and the difference signal was used to control the gain of the microwave system through a PIN diode

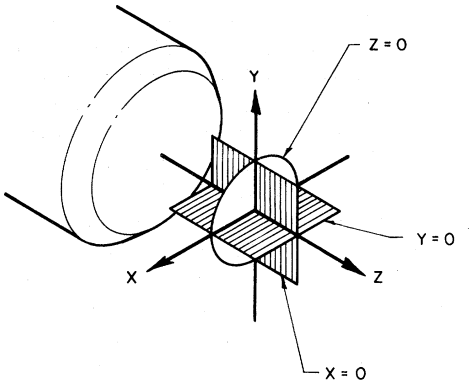

FIG. 4a. Coordinates for magnetic field plots. The origin of the coordinate system for field measurements was the center of the air gap. The z axis was the cylinder axis of the pole faces, the x axis was horizontal, and the y axis vertical.

modulator. The detector output was monitored with a digital voltmeter, and the system gain was occasionally adjusted by hand to keep the detector voltage within 0.1% of its value at the start of the pass through the resonance line. The detector was encased in insulation and shock mounted to minimize the effects of temperature variation and vibration on its characteristics. The temperature coefficient of the detector was 0.13%/°C and was found to be reproducible over the range of temperatures encountered in the experiment. Variations in ambient temperature during a pass were less than ±1.5 °C, so the change in power level due to temperature shifts was less than ±0.2%. The drift and the temperature effect were observed to be independent and can, therefore, be added in quadrature to give a combined upper limit on the

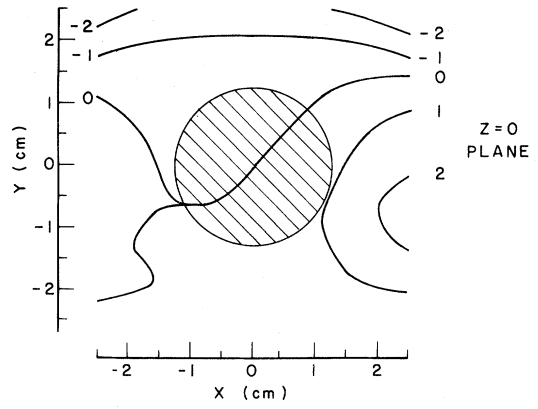

FIG. 4b. Magnetic field plot in $z = 0$ plane. Contours show deviation from central field in ppm. The hatched area in the center is the approximate region from which positronium annihilations are observed.

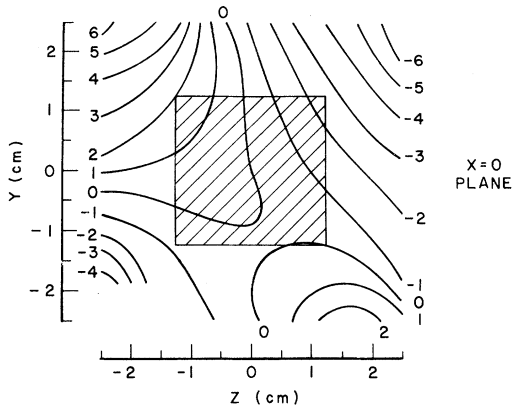

FIG. 4c. Magnetic field plot in $x = 0$ plane.

power stability of ±0.23%. A reasonable estimate of the standard deviation of the power level is ±0.12%.

A serious limitation on this and previous experiments was the failure of the gas to support high microwave fields at low pressure. As gas pressure was reduced, it was necessary to reduce the microwave field to prevent breakdown, until at some pressure the signal was too small to be usable. With nitrogen, higher breakdown fields are attainable than with the argon used in paper II, and positronium formation is comparable to that in other gases.[36] Useful data were taken at nitrogen pressures down to 0.27 atm.

C. Positron source

The source of positrons was 2.5 mCi of sodium-22 in the form of NaCl deposited in a brass source holder 10 mm in diam and 2 mm thick. The active material was deposited in an 8-mm-diam depression 1-mm-deep cut in one face of the holder and

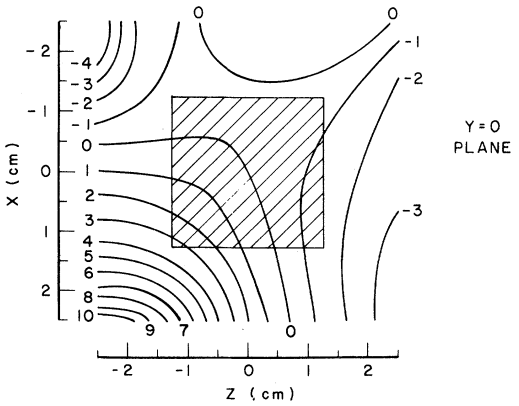

FIG. 4d. Magnetic field plot in $y = 0$ plane.

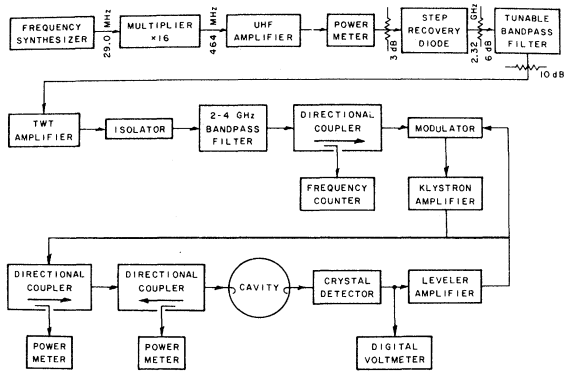

FIG. 5. Block diagram of the microwave system.

was sealed by a 0.006-mm-thick copper-foil window soldered to the holder.

D. Gas-handling system

A vacuum system consisting of a mechanical forepump, and oil diffusion pump,[37] and a thermoelectric cooled baffle[38] was used to evacuate the cavity. A pressure of 5×10^{-7} Torr was normally obtained at the diffusion pump which corresponded to a pressure of 3×10^{-5} Torr in the cavity allowing for the vacuum-line impedance.

All data were taken using ultrahigh purity nitrogen as the gas. The cylinder of gas was supplied[39] with the following analysis of impurities: O_2 – 2.2 ppm; moisture (H_2O) – 0.2 ppm; hydrocarbons <1 ppm. Gas pressure in the cavity was measured with a Bourdon tube gauge with a 0–100-lb/in^2, absolute, range and a 0.1-lb/in^2 accuracy.

E. γ-ray detectors and electronics

Eight γ-ray detectors were arranged as shown in Fig. 2 to provide four coincidence detectors for two collinear 0.51-MeV annihilation γ rays with 0.2-μsec time resolution. Each detector consisted of a 6.4-cm diam × 6.4-cm high NaI(Tl) scintillation crystal[40] coupled to a 7.6 cm photomultiplier tube[41] through a UVT acrylic light pipe, 6.4 cm in diam and 45.7-cm long. Concentric cylindrical shells of Netic and Co-Netic were used for magnetic shielding and resulted in a magnetic field at each photomultiplier tube of less than 0.25 G.

γ-ray shielding and collimation for the detectors was provided by lead blocks 17.8-cm thick with collimation slots which were 2.5-cm wide along the z axis and varied in height from 3.1 cm at the cavity to 5.0 cm at the detector. The dimensions were chosen so that the detectors could not see the positron source or its image on the opposite cavity wall.

Figure 7 shows the discriminator and coinci-

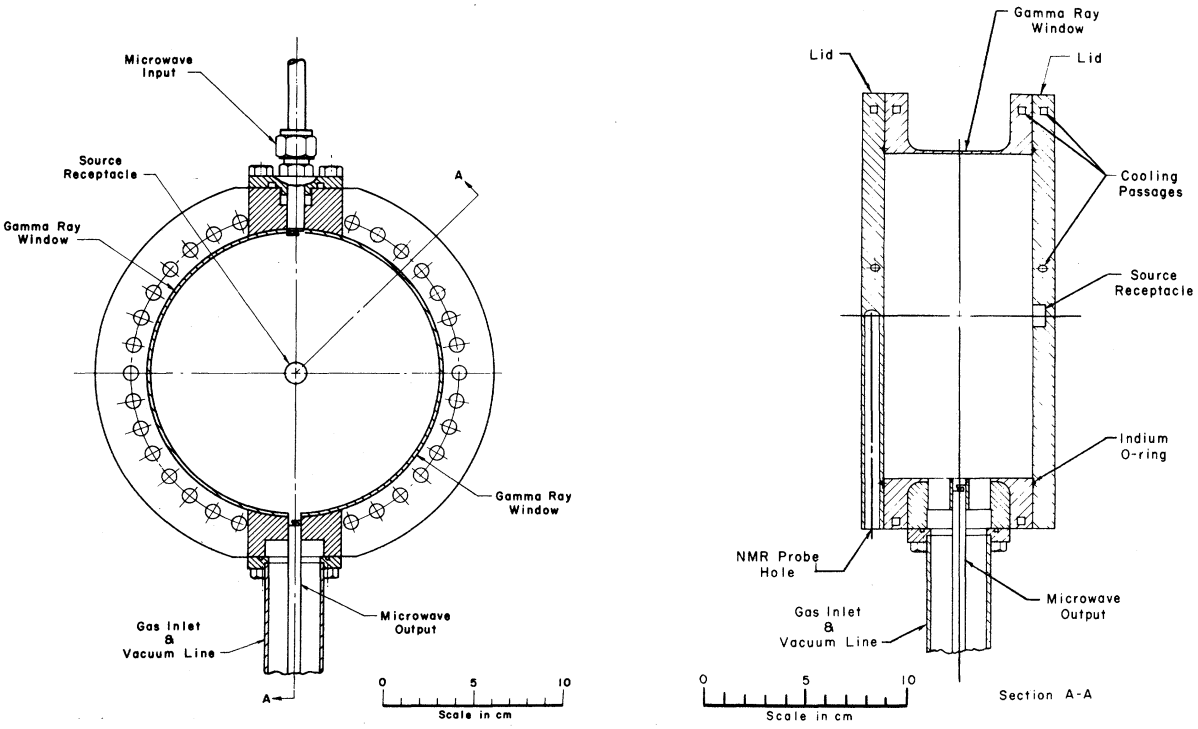

FIG. 6. Microwave cavity: (a) top view section, (b) side view section.

TABLE I. Average values of $\Delta\nu$ for each run.

Run	Pressure (atm)	H_1 (G)	$\Delta\nu$ (GHz)	σ (GHz)
1	0.27	13.3	203.3748	0.0093
2	2.72	13.3	203.3249	0.0227
3	0.34	13.4	203.3874	0.0087
4	0.27	11.9	203.4021	0.0103
5	0.68	13.4	203.3766	0.0099
6	0.68	16.8	203.3505	0.0150
7	1.36	16.8	203.3695	0.0260
8	0.14	8.3	203.4181	0.0307
9	0.27	10.7	203.3742	0.0098
10	1.36	17.2	203.3448	0.0095
11	1.70	17.2	203.3497	0.0105
12	0.31	12.7	203.3818	0.0047
13	0.31	12.9	203.3886	0.0071
14	2.18	17.2	203.3798	0.0211
15	2.59	16.5	203.3583	0.0106
16	3.40	16.5	203.3687	0.0128

dence circuits used with each coincidence pair, plus the routing logic and mixer necessary to store information from all four pairs in one multichannel pulse height analyzer. A pulse from detector B was gated into the multichannel analyzer and its amplitude stored when it was in coincidence with a pulse in the photopeak of detector *A*. The four pulse-height spectra accumulated in the multichannel analyzer were punched on paper tape, and for each coincidence detector the coincidence counting rate was determined by integrating the counts in the detector *B* photopeak with an off-line computer. The computer determined the integration limits as a function of the photopeak location in each spectrum, which allowed elimination of photomultiplier gain shifts and extraction of more information from the data. Typical coincidence count rates measured at the linear gate output varied from about 200 counts/sec to 1200 counts/sec over the range of experimental conditions. The corresponding rates at the linear gate input were 10 000 counts/sec and 15 000 counts/sec. The rate of accidental coincidences varied from about 6 counts/sec to 50 counts/sec and was 3–4% of the true coincidence rate.

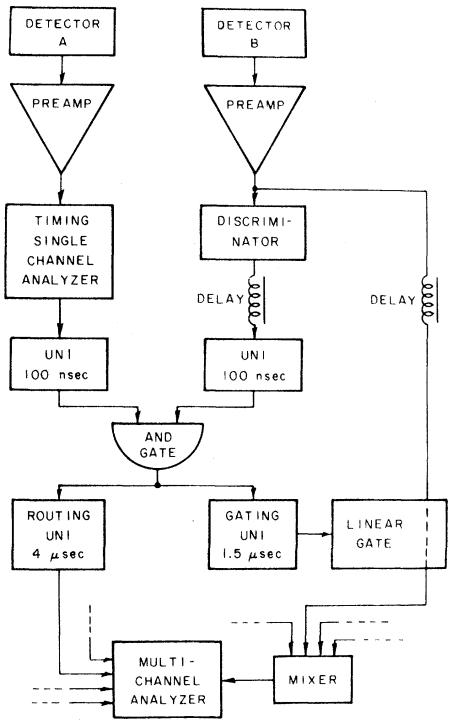

FIG. 7. Block diagram of coincidence detection circuit.

F. Experimental procedure

The following procedure was used to take data with the apparatus. The NMR frequency was set to the initial value for a pass through the positronium resonance, the magnetic field was brought into resonance with and locked to the NMR frequency, and accumulation of spectra by the multichannel analyzer was begun. When the accumulation was started, the data acquisition system punched the time, NMR frequency, and microwave frequency on the output paper tape. Accumulation continued for 20 min of multichannel-analyzer live time, after which the contents of the memory were punched on the tape. The 20 min live-time period was chosen because of the rather long time interval, almost 3 min, required to punch the entire analyzer memory on paper tape. While punchout was taking place, the magnetic field was set to the next value, and then after punching was completed, the analyzer memory was cleared, and the accumulation of spectra begun for the next field point.

A pass through the resonance consisted of taking data at the field points shown in the resonance curves of Fig. 8. The first and last points were far off the resonance to provide a measure of the background counting rate. At the end of a pass, a data point was taken at the initial field value to allow correction for drifts occurring during the pass. Data at the half-amplitude points of the resonance are effective for locating the line center, but a spread of points is needed to study the overall shape of the resonance line. About 6 h were required to complete a pass, and the total time for a pass was limited by slow drifts. At least every 5 days and usually when a different gas pressure was used, the cavity was evacuated and refilled to prevent accumulation of

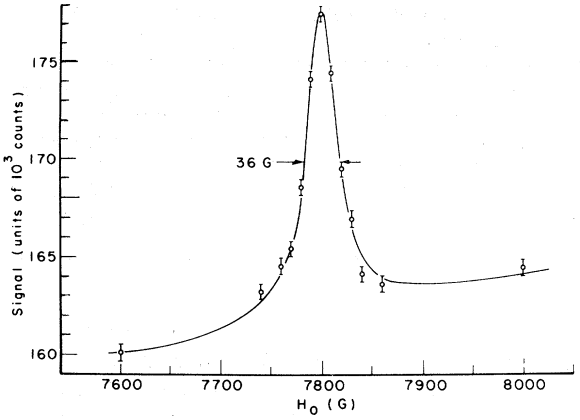

FIG. 8. Typical resonance line. Pressure = 0.31 atm N_2, f_{01} = 2 323.436 MHz.

outgassed contaminants.

Data were taken under various experimental conditions to test for systematic effects. The pressure was varied from 0.14 to 3.40 atm to measure the fine-structure density shift. At a fixed pressure, data were taken with the microwave magnetic field ranging from 7.6 to 9.4 G. Data were taken with the positron source on either side of the cavity to test for a geometry-dependent effect. Passes were taken with both increasing and decreasing magnetic-field values.

IV. DATA ANALYSIS

The raw data consisted of γ-ray energy spectra from the multichannel analyzer, one spectrum for each coincidence detector at each field point in a pass through the resonance.

The center of the photopeak in each coincidence spectrum was located by fitting the peak to a Tschebyscheff polynomial and finding the point of zero slope on the fitted curve. The number of counts in the photopeak was determined by summing over a range in the spectrum with the summation limits (expressed as a fraction of the photopeak center) corresponding to γ-ray energies of 0.46 and 0.59 MeV. This procedure of computing the summation limits as a function of the photopeak center reduced systematic changes in the observed counting rate due to gain shifts in the γ-ray detection apparatus.

The data were corrected for slow drifts in the apparatus which occurred over the period of a pass through the resonance. The count rates for the initial and final data points in the pass, which were taken at the same magnetic field, were compared, and the difference attributed to a drift linear in time occurring during the pass. Intervening data points were corrected according to this model.

The observed 2 γ-ray counts are principally contributed by free positron-electron annihilations, parapositronium annihilations, two γ-ray annihilations from $M=0$ orthopositronium, and annihilations of orthopositronium in collisions. The 2 γ-ray signal is principally due to microwave induced transitions from $M=\pm 1$ to $M=0$ orthopositronium, which lead to an increase in the number of 2 γ-ray annihilations. A resonance line is obtained by varying the magnetic field H_0. This results in a change in the background 2γ annihilations due to static magnetic field quenching of $M=0$ orthopositronium, i.e., the change in the $2\gamma/3\gamma$ branching ratio of the $M=0$ state of orthopositronium. Also, variation of H_0 changes the stopping distribution of positrons in the cavity and hence the number of 2γ annihilations viewed by the detectors. Estimates of the static magnetic field quenching indicate that it contributes $\approx 10\%$ of the observed change in background over the linewidth. The background 2γ annihilation rate is represented as linear in the magnetic field due to the small range of fields used. The expression fitted to the observed two-photon counting rate was

$$S'(H_0) = A_1(1 + A_2\Delta)(1 + A_3 S)\,, \tag{15}$$

in which S is the signal given by Eq. (12) or (13), A_1 is the amplitude of the background for $\Delta = 0$, A_2 is the slope of the background relative to A_1, A_3 is the amplitude of the signal relative to A_1, and Δ is the difference $H_0 - H_{0r}$ in units of the linewidth.

For each pass through the resonance, the corrected photopeak counts for each detector were separately fitted to the lineshape of Eq. (15) using the method of least squares, and a value for the magnetic field at the line center was thus obtained. Hence we calculate $\Delta\nu$ as follows:

$$\Delta\nu = \left(\frac{g'}{2(\mu_p'/\mu_B)}\right)^2 \frac{(f_p^c)^2}{f_{01}} - f_{01}\,, \tag{16}$$

in which f_p^c is the NMR frequency at the line center for a water sample, and[42] $\mu_p'/\mu_B = 1.520\,922\,983\,(17) \times 10^{-3}$. Equation (16) follows from Eq. (2).

The long computing time necessary to fit the complete theoretical lineshape to the data made analysis of all the experimental data using this lineshape prohibitively expensive. Instead, all the data were analyzed with the simple Lorentzian lineshape of Eq. (13), and only a selected sample of data at various gas pressures and microwave powers was analyzed with the complete theory of Eq. (12). Comparison indicated that $\Delta\nu$ obtained with Eq. (12) was 3.7 ± 0.3 MHz (or 18 ± 2 ppm)

lower than with Eq. (13), where the error quoted is the largest deviation observed for any pass in the sample of data. This correction factor was applied to the value of $\Delta\nu$ calculated using the simple theory.

A typical fitted line shape is shown in Fig. 8. The points are the measured counts with one standard deviation error bars. The solid line is the best fit of Eq. (15) where S is the Lorentzian line shape of Eq. (13). The difference in the fitted curve resulting from the use of the complete theory for S of Eq. (12) cannot be distinguished on the scale of Fig. 8. The error in $\Delta\nu$ determined from this typical resonance line was about 180 ppm and is overwhelmingly due to counting statistics.

A value of $\Delta\nu$ was determined for each detector pair for each pass through the resonance. The average of all $\Delta\nu$ values obtained in each run is computed, where a run is a set of passes taken continuously with the same gas pressure and microwave field. Table I presents these average values together with their statistical errors for all the data obtained.

A plot of the values of $\Delta\nu$ vs N_2 density is shown in Fig. 9. The solid circles are the weighted means of all values of $\Delta\nu$ obtained at a given density, and are shown with one standard deviation error bars, due predominantly to counting statistics. The data were fitted to the function

$$\Delta\nu(D) = \Delta\nu(0)(1 + aD) \tag{17}$$

for a linear fine structure density shift and to the function

$$\Delta\nu(D) = \Delta\nu(0)(1 + aD + bD^2)\,, \tag{18}$$

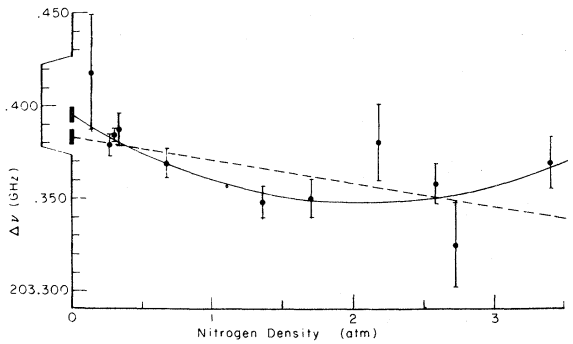

FIG. 9. Measured values of $\Delta\nu$ with one standard deviation errors vs N_2 density. The dashed line is the fit of Eq. (17) and the solid line is the fit of Eq. (18) to the measured points. The value of $\Delta\nu(0)$ for each fit is indicated by the bar.

TABLE II. Results of fits of the data $\Delta\nu(D)$ for N_2 gas to Eqs. (17) or (18).

Quantity	Linear fit	Quadratic fit
$\Delta\nu(0)$ (GHz)	203.384 ± 0.004	203.396 ± 0.005
a (10^{-5} atm^{-1} at 23 °C)	−5.7 ± 1.4	−23 ± 6
b (10^{-5} atm^{-2} at 23 °C)	0	+5.7 ± 1.8
χ^2/degrees of freedom	17.1/9	6.8/8

which includes a quadratic density shift as well. D is the gas density, and a and b are the linear and quadratic coefficients of the fine structure density shift, respectively. The results of these fits are given in Table II, and the fitted curves are shown in Fig. 9. The quadratic fit has a somewhat lower χ^2 than the linear fit, and hence was favored in our earlier brief publication on this experiment.[8] Unfortunately there are no theoretical calculations of a or b to aid in the choice. The linear fit does have a 5% probability of occurrence. However, the improved data of paper IV show that only a linear density shift is observed, and hence the linear fit in the present experiment is indeed the correct one. A study of the data indicates that runs 10 and 11 (Table II) gave the data points which most strongly suggested a quadratic density shift, and the log books indicated that these two runs were taken when the air conditioning system in the laboratory was not functioning normally. Otherwise there were no *a priori* reasons to reject these two runs. The values of $\Delta\nu(0)$ for the two fits shown in Table II differ by 11 MHz or by somewhat greater than two standard deviations.

A summary of the contributions to the error in $\Delta\nu$ is given in Table III corresponding to the choice of the linear fit. The total uncertainty in $\Delta\nu$ is $\sigma = 20$ ppm $= 4$ MHz and is due almost entirely to counting statistics.

TABLE III. Contributions to error in $\Delta\nu$ (in units of ppm).

Counting statistics, linear density shift fit	18
Magnetic field inhomogeneity	3.5
Magnetic field reproducibility and offset error	1.4
Correction between mineral oil and water NMR frequency	0.5
Microwave frequency stability and spectral purity	0.2
Microwave power stability	1.0
Correction for complete line shape theory	2.0
Total error (quadrature sum)	20 ppm

V. RESULTS

The principal result of our experiment is a value for $\Delta\nu$ of free positronium based on the linear density-shift fit of Eq. (17) to our data:

$$\Delta\nu_{\text{expt}} = 203.384 \pm 0.004 \text{ GHz (20 ppm)}, \quad (19)$$

in which the error is mainly a statistical counting error. The difference between the theoretical value for $\Delta\nu$ of Eq. (1) and the experimental value of Eq. (19) is

$$\Delta\nu_{\text{theor}} - \Delta\nu_{\text{expt}} = +20 \pm 4 \text{ MHz}, \quad (20)$$

where the uncertainty is the one standard deviation experimental error. A complete tabulation of all other measured values of $\Delta\nu$ and a discussion of the comparison with theory is given in paper IV.

Another result of our experiment is a value for the fine structure linear density shift of positronium in N_2 of Table II

$$a = -(5.7 \pm 1.4) \times 10^{-5} \text{ atm}^{-1} \text{ at } 23\,^{\circ}\text{C}. \quad (21)$$

---

*Research supported in part by the National Science Foundation (Grant GP 43847X).

†Present address: Bell Laboratories, Holmdel, N. J. 07733.

‡Present address: Physics Dept., Chalmers University of Technology, Gothenberg, Sweden.

[1]S. J. Brodsky and S. D. Drell, Ann. Rev. Nucl. Sci. 20, 147 (1970).

[2]B. E. Lautrup. A. Peterman, and E. deRafael, Phys. Reports 3, 193 (1972).

[3]V. W. Hughes, *Atomic Physics 3*, edited by S. J. Smith and G. K. Walters (Plenum, New York, 1973), p. 1.

[4]V. W. Hughes, *Physik 1973*, German Physical Society Conf. (Physik Verlag, Germany, 1973), p. 123.

[5]V. W. Hughes, S. Marder, and C. S. Wu, Phys. Rev. 106, 934 (1957). (Paper I of this series.)

[6]E. D. Theriot, Jr., R. H. Beers, V. W. Hughes, and K. O. H. Ziock, Phys. Rev. A 2, 707 (1970) (paper II).

[7]E. R. Carlson, V. W. Hughes, and I. Lindgren, Bull. Am. Phys. Soc. 17, 454 (1972).

[8]E. R. Carlson, V. W. Hughes, M. L. Lewis, and I. Lindgren, Phys. Rev. Lett. 29, 1059 (1972).

[9]P. O. Egan, W. E. Frieze, V. W. Hughes, and M. H. Yam, Phys. Lett. 54A, 412 (1975).

[10]P. O. Egan, V. W. Hughes, and M. H. Yam, following paper (paper IV), Phys. Rev. A 15, 251 (1977).

[11]R. Karplus and A. Klein, Phys. Rev. 87, 848 (1952).

[12]T. Fulton, D. A. Owen, and W. W. Repko, Phys. Rev. A 4, 1802 (1971).

[13]D. A. Owen, Phys. Rev. Lett. 30, 887 (1973).

[14]R. Barbieri, P. Christillin, and E. Remiddi, Phys. Rev. A 8, 2266 (1973).

[15]P. T. Olsen and E. R. Williams, *Atomic Masses and Fundamental Constants 5*, edited by J. H. Sanders and A. H. Wappstra, (Plenum, New York, 1976), p. 538.

[16]T. W. Hänsch, M. H. Nayfeh, S. A. Lee, S. M. Curry, and I. S. Shahin, Phys. Rev. Lett. 32, 1336 (1974).

[17]E. R. Cohen and B. N. Taylor, J. Phys. Chem. Ref. Data 2, 663 (1973).

[18]M. L. Lewis and V. W. Hughes, Phys. Rev. A 8, 625 (1973).

[19]E. R. Carlson, Ph.D. thesis (Yale University, 1971) (unpublished).

[20]H. Grotch and R. Kashuba, Phys. Rev. A 7, 78 (1973).

[21]P. Cvitanovic and T. Kinoshita, Phys. Rev. D 10, 4007 (1974).

[22]A. Rich and J. C. Wesley, Rev. Mod. Phys. 44, 250 (1972).

[23]I. Harris and L. M. Brown, Phys. Rev. 105, 1656 (1957).

[24]M. A. Stroscio, Phys. Rev. A 12, 338 (1975).

[25]G. J. Celitans and J. H. Green, Proc. Phys. Soc. 83, 823 (1964).

[26]Varian Model V-3802 15-inch electromagnet with model V-FR2703 power supply and Mark II Fieldial Regulator.

[27]W. H. Wing, E. R. Carlson, and R. J. Blume, Rev. Sci. Instr. 41, 1303 (1970).

[28]Nujol extra heavy mineral oil.

[29]S. A. Lewis, Ph.D. thesis (Yale University, 1969) (unpublished).

[30]H. S. Gutowsky and R. E. McClure, Phys. Rev. 81, 276 (1951).

[31]S. Liebes, Jr., and P. Franken, Phys. Rev. 116, 633 (1959).

[32]E. R. Andrew, *Nuclear Magnetic Resonance* (Cambridge U. P., Cambridge, 1955).

[33]Hewlett-Packard Model 5100A/5110A frequency synthesizer.

[34]Varian Model VA-802B.

[35]R. Beringer, in *Technique of Microwave Measurements*, edited by C. G. Montgomery (Dover, New York, 1966), Vol. I, Chap. 5, p. 299.

[36]T. A. Pond, Phys. Rev. 85, 489 (1952).

[37]Norton NRC Model HS-2.

[38]Edwards High Vacuum Model DCB2A.

[39]Linde Division of Union Carbide Corp.

[40]Harshaw Model 10D10.

[41]RCA Model 4524.

[42]W. D. Phillips, W. E. Cooke, and D. Kleppner, Phys. Rev. Lett. 35, 1619 (1975).